

THE LAGRANGE EQUILIBRIUM POINTS L_4 AND L_5 IN A BLACK HOLE BINARY SYSTEM

JEREMY D. SCHNITTMAN

Department of Physics and Astronomy, Johns Hopkins University, Baltimore, MD 21218

Draft version October 22, 2018

ABSTRACT

We calculate the location and stability of the L_4 and L_5 Lagrange equilibrium points in the circular restricted three-body problem as the binary system evolves via gravitational radiation losses. Relative to the purely Newtonian case, we find that the L_4 equilibrium point moves towards the secondary mass and becomes slightly less stable, while the L_5 point moves away from the secondary and gains in stability. We discuss a number of astrophysical applications of these results, in particular as a mechanism for producing electromagnetic counterparts to gravitational-wave signals.

Subject headings: black hole physics – relativity – gravitational waves – galaxies: nuclei

1. INTRODUCTION

Recent advances in numerical relativity (NR) have led to an increasing interest in the astrophysical implications of black hole (BH) mergers. Of particular interest is the possibility of a distinct, luminous electromagnetic (EM) counterpart to a gravitational wave (GW) signal (Bloom et al. 2009). If such an EM counterpart could be identified with a LISA¹ detection of a supermassive BH binary in the merging process, then the host galaxy could likely be determined. A large variety of potential EM signatures have recently been proposed, almost all of which require some significant amount of gas in the near vicinity of the merging BHs.

Gas in the form of accretion disks around single massive BHs is known to produce some of the most luminous objects in the universe. However, very little is known about the behavior of accretion disks around *two* BHs, particularly at late times in their inspiral evolution. In Newtonian disks, it is believed that a circumbinary accretion disk will have a central gap of much lower density, either preventing accretion altogether, or at least decreasing it significantly (Pringle 1991; Artymowicz & Lubow 1994, 1996). When including the evolution of the binary due to GW losses, the BHs may also decouple from the disk at the point when the GW inspiral time becomes shorter than the gaseous inflow time at the inner edge of the disk (Milosavljevic & Phinney 2005). This decoupling should effectively stop accretion onto the central object until the gap can be filled on an inflow timescale. However, other semi-analytic calculations predict an enhancement of accretion power as the evolving binary squeezes the gas around the primary BH, leading to a rapid increase in luminosity shortly before merger (Armitage & Natarajan 2002; Chang et al. 2009).

Setting aside for the moment the question of *how* the gas can or cannot reach the central BH region, a number of recent papers have shown that *if* there is sufficient gas present, then an observable EM signal is likely. Krolik (2010) used analytic arguments to estimate a peak luminosity comparable to that of the Eddington limit, independent of the detailed mechanisms for shocking and heating the gas. Using relativistic

magneto-hydrodynamic simulations in 2D, O’Neill et al. (2009) showed that the prompt mass loss due to GWs actually leads to a sudden *decrease* in luminosity following the merger, as the gas in the inner disk temporarily has too much energy and angular momentum to accrete efficiently. Full NR simulations of the final few orbits of a merging BH binary have now been carried out including the presence of EM fields in a vacuum (Palenzuela et al. 2009; Mosta et al. 2010; Palenzuela et al. 2010) and also gas, treated as test particles in van Meter et al. (2010) and as an ideal fluid in Bode et al. (2010) and Farris et al. (2010). The simulations including matter all suggest that the gas can get shocked and heated to high temperatures, thus leading to bright counterparts in the event that sufficient gas is in fact present. One estimate of “sufficient” is the condition that the gas be optically thick to electron scattering, which will lead to Eddington-rate luminosities (Krolik 2010). Thus we require $\kappa\rho R \gtrsim 1$, where $\kappa = 0.4 \text{ cm}^2\text{g}^{-1}$ is the opacity and ρ is the characteristic density over a length scale $R \sim 10 GM_{\text{BH}}/c^2$. Then the total mass is a modest $M_{\text{gas}} \sim \rho R^3 \approx 5 \times 10^{26} M_7^2 \text{ g}$, where $M_7 = M_{\text{BH}}/(10^7 M_\odot)$. More gas will generally lead to longer, but not necessarily more luminous signals.

The motivation for this work is to understand potential dynamical processes that could lead to a significant amount of gas around the BHs at the time of merger. We focus on stable orbits in the circular, restricted three-body problem, i.e., a system with two massive objects orbiting each other on circular, planar Keplerian orbits, with the third body being a test particle free to move out of the plane. Gas or stars that get captured into these stable regions at large binary separation may remain trapped as the binary orbit shrinks due to radiation reaction. In this paper, we integrate the restricted three-body equations of motion in the corotating frame for a range of BH mass ratios, including the evolution of the binary with leading-order post-Newtonian GW losses. With the exception of these non-conservative corrections, all dynamics are considered at the purely Newtonian level.

We find that particles initially close to the L_4 and L_5 Lagrange points remain on stable orbits throughout the adiabatic evolution of the BH binary. This result imme-

¹ <http://lisa.nasa.gov>

diately leads to a number of astrophysical predictions. If diffuse gas is captured from the surrounding medium, and irradiated by an accretion disk around either BH, it may produce strong, relatively narrow emission lines with large velocity shifts, varying on an orbital time scale. If individual stars are captured, they may eventually get tidally disrupted by one of the BHs shortly before merger, providing an enormous source of material for accretion. Stars may also get ejected from the system at late times, producing ultra-hyper-velocity stars moving away from the galactic center at a significant fraction of the speed of light. Clusters of stars could also get captured or form *in situ* at large binary separation, then get compressed adiabatically as the BH system shrinks, ultimately collapsing from gravitational instabilities. Compact objects such as neutron stars or stellar-mass BHs would not get tidally disrupted in most cases, but could still possibly be detected with LISA as perturbations to the GW signal.

While this manuscript was in preparation, a similar work by Seto & Muto (2010) was published, with some of the same conclusions. One major distinction is that they included first-order post-Newtonian terms in their equations of motion, while we do not. Also, they “have not found notable qualitative differences” between L_4 and L_5 , while we do. Many of our astronomical predictions are qualitatively similar, but have been derived independently.

The outline for this paper is as follows: in Section 2 we present the three-body equations of motion, including GW losses, and analyze the stability and location of the equilibrium Lagrange points. These analytic predictions are tested in Section 3 with numerical simulations of a large number of test particles. In Section 4 we explore in more detail some potential astronomical applications of these results, and in Section 5 we conclude.

2. LOCATION AND EVOLUTION OF STABLE LAGRANGE POINTS

We consider a three-body system wherein the larger bodies have masses M_1 and M_2 ($M_1 > M_2$; $M \equiv M_1 + M_2$) and the third object is a test particle of negligible mass m_0 . We define dimensionless masses $\mu_1 \equiv M_1/M$ and $\mu_2 \equiv M_2/M$. M_1 and M_2 move on circular, Keplerian orbits around the center of mass at the origin with semi-major axis $a(t)$. Unless otherwise stated, we use geometrized units with $G = M = c = 1$. In the corotating frame we define coordinates (x, y, z) , with the primary BH located at $(-\mu_2 a, 0, 0)$ and the secondary at $(\mu_1 a, 0, 0)$. The angular velocity of the system in the lab frame is $n = a^{-3/2}$. The binary is orbiting in the $+\phi$ direction for the standard definition of spherical coordinates. The equations of motion for the test particle may be written as

$$\ddot{x} = 2n\dot{y} + n^2x + \dot{n}y - \left[\mu_1 \frac{x + a\mu_2}{r_1^3} + \mu_2 \frac{x - a\mu_1}{r_2^3} \right] \quad (1a)$$

$$\ddot{y} = -2n\dot{x} + n^2y - \dot{n}x - \left[\frac{\mu_1}{r_1^3} + \frac{\mu_2}{r_2^3} \right] y \quad (1b)$$

$$\ddot{z} = - \left[\frac{\mu_1}{r_1^3} + \frac{\mu_2}{r_2^3} \right] z \quad (1c)$$

$$\dot{n} = \frac{96}{5} \mu_1 \mu_2 n^{11/3}, \quad (1d)$$

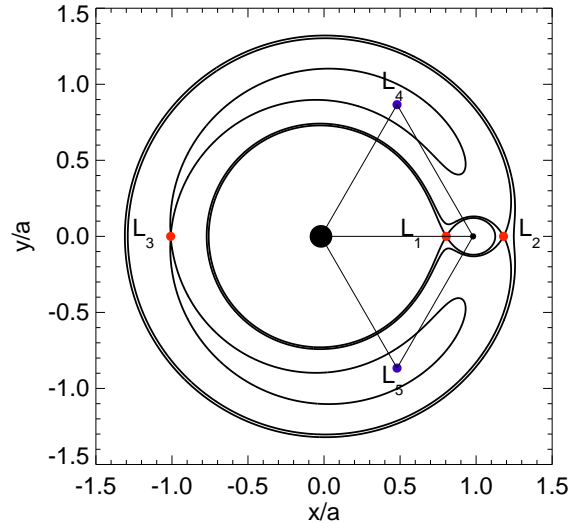


Figure 1. Contours of the Jacobi constant C_{J0} for test particles at rest in the rotating frame, for secondary mass $\mu_2 = 0.02$. The stable Lagrange points L_4 and L_5 are located at local minima of C_{J0} , and form equilateral triangles with the two massive bodies. The co-linear Lagrange points L_1 , L_2 , and L_3 are located at saddle-points of C_{J0} and are unstable equilibrium points. The x - and y -axes have been normalized to the binary separation a .

where r_1 and r_2 are the distances to the primary and secondary bodies, respectively. These reproduce the classical Newtonian system in the limit of $\dot{n} \rightarrow 0$, i.e. when gravitational radiation reaction is turned off.

It is well-known from classical mechanics that there exist five equilibrium points where a test particle can remain at rest in the corotating frame ($\ddot{x} = \ddot{y} = \ddot{z} = 0$) (Murray & Dermott 1999). These points are known as the Lagrange equilibrium points ($L_1 \dots L_5$), and are plotted in Figure 1 for a binary with mass ratio $\mu_2 = 0.02$. The co-linear points L_1 , L_2 , and L_3 are always unstable, while the triangular points L_4 and L_5 are linearly stable only for $\mu_2 \lesssim 0.0385$ (Murray & Dermott 1999). In the Newtonian problem, there is a single integral of motion, the Jacobi constant:

$$C_J \equiv n^2(x^2 + y^2) + 2 \left(\frac{\mu_1}{r_1} + \frac{\mu_2}{r_2} \right) - \dot{x}^2 - \dot{y}^2 - \dot{z}^2. \quad (2)$$

Setting the particle’s velocity to zero in the corotating frame, the contours of constant $C_{J0} \equiv C_J(v = 0)$ in the $x - y$ plane define “zero velocity curves,” as plotted in Figure 1. L_4 and L_5 are located at local minima of C_{J0} , while L_1 , L_2 , and L_3 are saddle-points (note that C_J has the form of a negative energy, so that local minima are actually points of maximum potential energy, yet are still stable to small perturbations because of the restoring Coriolis forces in the rotating frame). One well-known implication of this feature is that gas bound to either M_1 or M_2 can pass through L_1 and subsequently accrete onto the other object, a process known as mass transfer in standard stellar binary evolution. Additionally, any particle with $C_J > C_{J0}(L_3)$ would be excluded from crossing into the tadpole-shaped regions around L_4 and L_5 .

Murray (1994) explore the effects of generalized non-

gravitational forces acting on test particles in the restricted three-body problem, including a detailed study of how the position and stability of the Lagrange equilibrium points are affected. At first glance, our problem would seem quite similar, with the \dot{n} terms in equations (1a),(1b) acting as pseudo-drag forces: as the binary orbit shrinks and n increases, test particles would feel like they are accelerating in the $-\phi$ direction in the corotating frame, thus slowing down in the inertial frame. In this case, Murray (1994) show that L_4 and L_5 both move in the $+\phi$ direction, thus compensating for the inertial drag and still maintaining $\ddot{x} = \ddot{y} = 0$. However, when considering the time-varying nature of n and a in equations (1a)-(1d) due to GW losses, we find that this drag force analogy breaks down. Numerical integration of equations (1a)-(1d) show that in fact, the opposite occurs, with L_4 and L_5 moving in the $-\phi$ direction in the rotating frame.

Remarkably, this result can still be understood via an inertial drag term, if one applies it not to the test particle, but to the secondary mass. In order to study the evolution of the Trojan asteroids under the influence of a radial migration by Jupiter, Fleming & Hamilton (2000) apply an artificial drag force that acts only on Jupiter in the form $\mathbf{F} = -k\mathbf{v}$ in the inertial frame. Of course, this causes the secondary to lose energy and angular momentum and thus orbit faster, increasing n as in the BH binary case. Since there is no requirement on the relative masses of the secondary M_2 and the test particle m_0 to ensure stability of L_4 and L_5 (Salo & Yoder 1988), we can in fact adopt the drag force analysis of Murray (1994) to include GW losses by reversing the roles of the secondary BH and the test particle. In the rotating frame, the inertial drag force is given by $F_x = -k(x - ny)$ and $F_y = -k(\dot{y} + nx)$. For stationary particles at the equilibrium points, equations (1a),(1b) become

$$\bar{k}ny = -n^2x + \left[\mu_1 \frac{x + a\mu_2}{r_1^3} + \mu_2 \frac{x - a\mu_1}{r_2^3} \right] \quad (3a)$$

$$\bar{k}nx = n^2y - \left[\frac{\mu_1}{r_1^3} + \frac{\mu_2}{r_2^3} \right] y, \quad (3b)$$

where $\bar{k} = k/m_0$, and we have replaced the GW acceleration terms $\dot{n}y$ and $\dot{n}x$ with those appropriate for drag forces F_x/m_0 and F_y/m_0 .

In order to reproduce the GW evolution of equation (1d), we must choose the magnitude of the drag force appropriately. This is done by equating the energy loss due to the shrinking orbit with that of the inertial drag force. For circular Keplerian orbits, we have

$$\dot{E}_{\text{drag}} = \mathbf{F} \cdot \mathbf{v} = -kv^2 = -kn^2/3 \quad (4)$$

and

$$\dot{E}_{\text{orbit}} = \frac{d}{dt} \left(-\frac{m_0}{2a} \right) = -\frac{m_0}{3} n^{-1/3} \dot{n}. \quad (5)$$

Equating (4) and (5), along with (1d) allows us to solve for \bar{k} :

$$\bar{k} = \frac{1}{3} \frac{\dot{n}}{n} = \frac{32}{5} \mu_1 \mu_2 n^{8/3}. \quad (6)$$

Following Murray (1994), we multiply equation (3a) by

y and add to (3b) times x , giving

$$\bar{k}nr^2 = \mu_1 \mu_2 ay \left(\frac{1}{r_1^3} - \frac{1}{r_2^3} \right). \quad (7)$$

In the limit of small μ_2 , $a \approx r \approx r_1$ at the stable Lagrange points and we can write

$$\bar{k} \approx \frac{\mu_1 \mu_2}{na^3} \sin \phi_L \left(1 - \frac{1}{(2 - 2 \cos \phi_L)^{3/2}} \right), \quad (8)$$

where ϕ_L is the location of the Lagrange point in the presence of an inertial drag force. When considering the orbital evolution due to GW losses, we can use equation (6) for \bar{k} . We must also reverse the sign of ϕ_L because, as mentioned above, the GW drag force is really applied to M_2 and not to the test particle as in Murray (1994). We now have an expression for the location of the Lagrange points in the presence of GW losses:

$$\sin \phi_L \left(\frac{1}{(2 - 2 \cos \phi_L)^{3/2}} - 1 \right) = \frac{32}{5} a^{-5/2}. \quad (9)$$

This relation is plotted as a dashed curve in Figure 2. Interestingly, to leading order, the location of the Lagrange points is a function only of the binary orbital separation, *not* the mass ratio, even though the inspiral timescale is strongly dependent on μ_2 . Note that, when including non-conservative forces such as GW evolution, there is a lack of symmetry between L_4 and L_5 , with L_4 moving towards the secondary mass, while L_5 moves away from it. We also find differences in the relative stability of orbits around each Lagrange point, as described in the next section.

3. NUMERICAL TESTS

In Figure 2 we plot the position of test particles near L_4 and L_5 as a function of the binary separation a for a range of mass ratios. The initial binary separation is $a_0 = 40M$. For the most part, the test particles remain very close to their initial locations throughout inspiral, evolving according to equation (9). While our Newtonian equations of motion do not formally predict an innermost stable circular orbit (ISCO), we expect the BHs to plunge and merge around $a = 5M$, at which point very little evolution in ϕ_L has taken place. The slight offsets in the various curves at large a are due to the fact that ϕ is measured with respect to the origin, not M_1 . The inclusion of post-Newtonian (PN) corrections to the equations of motion would likely change the shape of the curves in Figure 2 slightly, as well as the detailed shape of stability regions around L_4 and L_5 (Rosswog & Trautman 1996). It should be noted that Seto & Muto (2010) include only 1PN terms, and do find a significant reduction in stability for certain mass ratios. Yet due to the notoriously uneven convergence of most PN expansions (e.g. Buonanno et al. (2009) and references therein), it is not clear whether their inclusion would add significant physical insight to the problem.

When studying inertial drag forces such as those described above, Murray (1994) found that the L_4 point was more stable than L_5 . Since our problem is the mirror-image of that one, it is not surprising then that we find greater stability around L_5 when including GW evolution. As shown in the upper panel of Figure 2 for

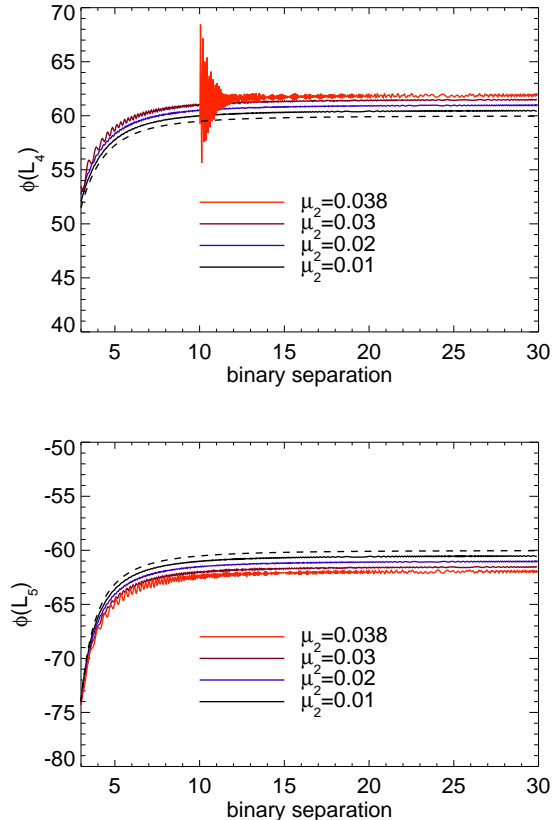


Figure 2. *Upper:* The location of test particles initially at rest near the L_4 Lagrange point in the rotating frame. As the binary system evolves to smaller separation a , the L_4 point moves towards the secondary BH, located at $\phi = 0$. For $\mu_2 = 0.038$, L_4 becomes linearly unstable around $a = 15M$, and the test particle is ejected at $a = 10M$. *Lower:* The location of test particles initially at rest near the L_5 Lagrange point. Towards the end of the BH inspiral, the L_5 point moves *away* from the secondary. In both figures, we plot the analytic prediction of equation (9) as a dashed curve.

$\mu_2 = 0.038$, a test particle initially very close to L_4 will eventually get ejected from the equilibrium configuration as the binary approaches merger. On the other hand, test particles librating around L_5 appear to become *more* stable, asymptotically approaching the exact equilibrium position. As mentioned in Erdi et al. (2009), for binaries with μ_2 slightly above the critical value for linear stability ($0.0385 \lesssim \mu_2 \lesssim 0.0401$), there still exist bound orbits that librate around L_4 and L_5 with moderate amplitude. We find that for these systems, the inclusion of radiation reaction increases the stability of L_5 by damping the libration amplitude. On the other hand, the libration amplitude of particles around L_4 grows rapidly towards the end of inspiral, as in the linear case in Figure 2. In contrast, Seto & Muto (2010) find no difference between L_4 and L_5 , although they only consider a few test particles around each Lagrange point.

To further investigate this asymmetry in stability, we carried out orbital integrations for large numbers of test particles distributed in clouds around each Lagrange point for masses $\mu_2 = 0.01, 0.02$, and 0.038 . This allowed us to probe the regions relatively far from the equilibrium points, where standard linear stability analysis breaks down. We used two methods for estimating

the large-scale stability of orbits around each Lagrange point. The first was a simple number count: the fraction of particles that remain bound around the equilibrium point. In this context, a particle is considered bound if its instantaneous Jacobi constant C_J is less than $C_{J0}(L_3)$ for the present orbital separation, corresponding to the tadpole-shaped regions around L_4 and L_5 in Figure 1. Additionally, any particle that escapes with $r > 10a$ or approaches closer than $3\mu_1$ from the primary or $3\mu_2$ from the secondary is removed from the system. The second method of measuring stability was to calculate the total volume filled by bound particles around each Lagrange point. A larger volume corresponds to lower stability, as the particles begin to escape the bound libration region.

The fraction of bound particles f_{bound} is plotted in the top panels of Figure 3, normalized to the bound number at binary separation of $a = 35M$. The particles begin in a small cloud of radius δR around each Lagrange point with random velocities, isotropic with $\langle v \rangle = v_{\text{orb}}(\delta R/a)^{1/2}$ in the corotating frame. We select δR to be large enough so that the cloud of particles roughly fills the phase-space volume of stable orbits around L_4 and L_5 . In practice, this typically corresponds to half of the particles getting ejected on roughly a dynamical time after the start of the simulation (hence f_{bound} is defined relative to $a = 35M$, not $a = 40M$). After a stable cloud is formed around each Lagrange point, marginally bound particles are slowly ejected from the system (or accreted onto one of the BHs) as the binary system evolves adiabatically. From Figure 2, we might expect more particles to get ejected from L_4 , which appears to be less stable, at least at linear order. However, as evident in Figure 3, L_4 retains more bound particles when $\mu_2 = 0.01$, L_5 appears more stable for $\mu_2 = 0.02$, and they are nearly identical for $\mu_2 = 0.038$.

It is not entirely clear why this peculiar behavior occurs, with no apparent trend in global stability as a function of mass ratio, nor why one Lagrange point or the other should be more stable for a given mass ratio. As described in Murray & Dermott (1999), test particles near the stable Lagrange points move along epicycles with two distinct frequencies. For certain values of μ_2 , these libration frequencies have integer commensurabilities, which naturally leads to strong resonant interactions (Deprit & Deprit-Bartholomé 1967). For example, when $\mu_2 = 0.0243$, both L_4 and L_5 are stable under standard linear analysis, yet the two epicyclic frequencies have a ratio of $2 : 1$, leading to resonant excitations and ejection of all test particles after a few dynamical times (Erdi et al. 2009; Seto & Muto 2010). Murray (1994) shows that these characteristic frequencies change in the presence of inertial drag forces, which we have shown above to be directly analogous to GW evolution. Thus we suspect that the different behavior seen in $f_{\text{bound}}(t)$ for different Lagrange points is due to a combination of resonant interactions and asymmetric shifts in the libration frequencies due to the binary evolution via GW losses.

In the bottom panels of Figure 3 we plot the total volume V_{bound} occupied by bound particles, normalized to the overall scale of the binary a^3 . In the limit of a very small $\delta R/a$, where the test particles are well within the linear regime, the cloud around each Lagrange

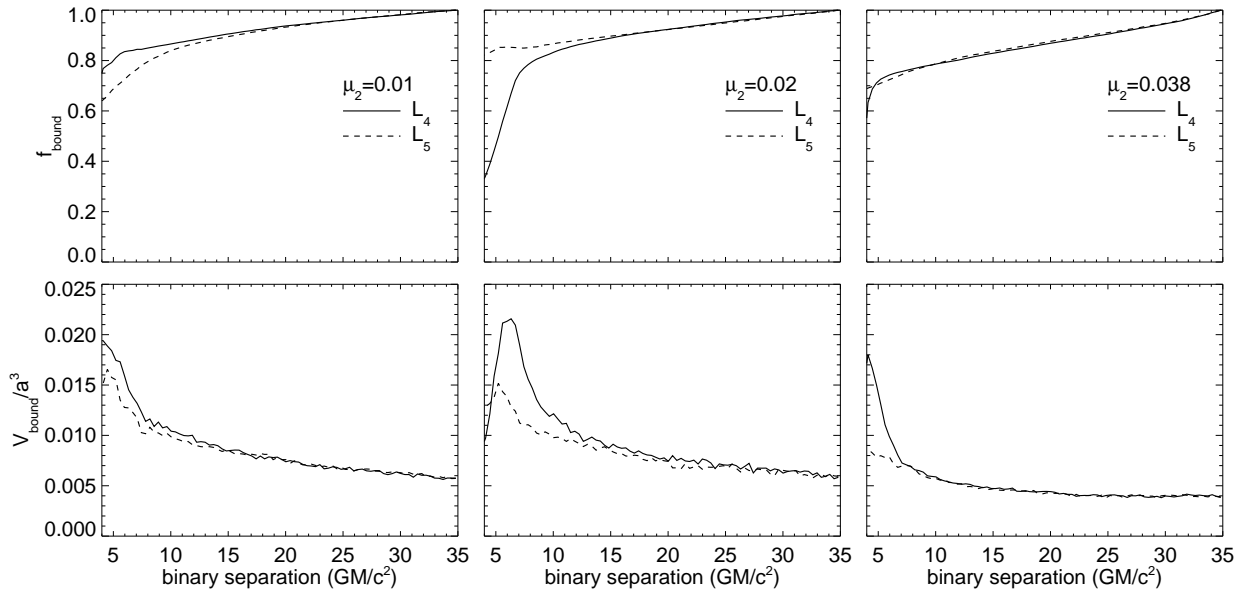


Figure 3. *Upper:* The fraction f_{bound} of test particles that remain bound in librating orbits around L_4 (solid curves) and L_5 (dashed curves) for a range of mass ratios. The particles are initially distributed in a small cloud around each Lagrange point with binary separation $a = 40M$. f_{bound} is normalized to the number of bound particles when $a = 35M$. *Lower:* The volume of space occupied by bound test particles around L_4 (solid curves) and L_5 (dashed curves), normalized by the characteristic volume of the system, a^3 .

point will actually expand adiabatically relative to the binary separation, although shrinking on an absolute scale. Fleming & Hamilton (2000) show this evolution to scale as $a^{9/4}$:

$$\left(\frac{V_f}{V_i}\right) = \left(\frac{a_f}{a_i}\right)^{9/4}, \quad (10)$$

where V_i and V_f are the initial and final volumes of test particle clouds. We have confirmed this result numerically with simulations starting with $\delta R \ll a$. On the other hand, if $\delta R/a$ is large enough such that the stable region of phase space is completely filled, the normalized volume V/a^3 should be constant, since the entire problem is scale-invariant. Any adiabatic expansion will not increase the volume of bound orbits, but rather decrease the total number of particles in these regions, as seen in the upper panels of Figure 3.

We actually find a gradual increase in V_{bound}/a^3 as the binary shrinks, yet still much slower than the Fleming & Hamilton (2000) result of $(V/a^3) \sim a^{-3/4}$, suggesting that the bound region in phase space is in fact filled. The increase in V_{bound}/a^3 during the adiabatic inspiral phase ($a \gtrsim 10M$) is likely due to a combination of effects. First, we expect a net increase in global stability caused by the GW losses, analogous to the effects of inertial drag described above. Secondly, there is also some inherent error in measuring the volume of bound orbits, based on our crude metric of the test particles' instantaneous Jacobi constants. Some fraction of particles that have moved outside the stable region may still appear bound for a few dynamical times before getting ejected or accreted, and thus artificially contribute to V_{bound} . At smaller a , where the libration time becomes comparable to the inspiral time, the system no longer evolves adiabatically, and a cloud of particles can get “frozen” at roughly constant volume, leading to the rapid increase in V_{bound}/a^3 for $a \lesssim 10M$. Interestingly, we do see a

consistent trend of larger V_{bound} around L_4 than L_5 for all values of μ_2 , as suggested by Figure 2. However, this may be less a measure of local stability than a consequence of the fact that L_4 moves *toward* the secondary, while L_5 moves away from it. Thus the two regions begin to sample different potentials, and the gravitational force of the secondary acts to disrupt the cloud around L_4 more strongly than that around L_5 , in turn leading to a larger V_{bound} .

We should add as a word of caution, that many of these numerical stability results may be altered somewhat by the inclusion of additional PN terms to the equations of motion (Seto & Muto 2010). In general relativity, unlike the case of Newtonian gravity, test particles moving in the Kerr metric have three distinct epicyclic frequencies. These additional frequencies may lead to more complicated resonant interactions and thus change the behavior of $f_{\text{bound}}(a)$ and $V_{\text{bound}}(a)$, at least at a quantitative level. Yet our intuition suggests that the *qualitative* behavior shown in Figure 3 should remain unchanged. Future work will investigate this question in greater detail.

4. ASTROPHYSICAL APPLICATIONS

4.1. Formation Mechanisms

In the previous Sections, we showed analytically and numerically how the location and stability of the L_4 and L_5 Lagrange points evolve in the presence of radiation reaction. We found that test particles, once captured into libration orbits around one of the stable Lagrange points, will in general remain there throughout the adiabatic inspiral phase, as the entire length scale of the system steadily shrinks. However, the initial premise was not addressed: will there even be gas or stars or debris present in the first place? How might matter get captured into these orbits at large binary separations of $a \gtrsim 1$ pc? Furthermore, are binary BHs with $\mu_2 \lesssim 0.04$ astrophysically likely, or even possible?

Even in a system as well-studied as the Sun-Jupiter binary, there is still no clear consensus on the origin of the Trojan asteroids, despite the fact that orbital elements are now known for over 4000 individual objects. Rabe (1972) proposed that they may be captured comets, while Shoemaker et al. (1989) and Kary & Lissauer (1995) suggested a more local origin as planetesimals in the early solar system. In most theories, some form of dissipative force is required to capture the Trojans (Yoder 1979), such as nebular gas drag (Murray 1994; Kary & Lissauer 1995) or planetesimal collisions (Shoemaker et al. 1989). Additionally, an increase in Jupiter’s mass via accretion of the surrounding disk could lead to asteroids getting captured (Marzari & Scholl 1998; Fleming & Hamilton 2000). Analogous to our BH binary system, the inward migration of Jupiter may have also affected the capture and subsequent evolution of the Trojans (Yoder 1979; Fleming & Hamilton 2000).

The characteristic separation at which point a hard BH binary (i.e., the orbital potential is dominated by the two BHs, and not by the surrounding stars) is formed is comparable to the primary BH’s radius of influence (Merritt 2006):

$$a_h = \frac{q}{(1+q)^2} \frac{R_{\text{infl}}}{4}, \quad (11)$$

where $q = M_2/M_1$ and

$$R_{\text{infl}} = \frac{GM}{\sigma^2} \approx 1.1 \text{ pc} \left(\frac{M}{10^7 M_\odot} \right) \left(\frac{\sigma}{200 \text{ km s}^{-1}} \right)^{-2}, \quad (12)$$

with σ being the one-dimensional velocity dispersion of the galaxy’s bulge. In the limit of small $\mu_2 \approx q \ll 1$, we have

$$a_h \approx 5 \times 10^{-3} \text{ pc} \left(\frac{\mu_2}{0.02} \right) \left(\frac{M}{10^7 M_\odot} \right) \left(\frac{\sigma}{200 \text{ km s}^{-1}} \right)^{-2}, \quad (13)$$

corresponding to $a_h \sim 10^4 M$ in geometrized units. Within this region, there are typically thousands of stars (Hopman & Alexander 2006), and in active galactic nuclei (AGN), a great deal of gas and dust as well. It is also roughly the separation at which point the binary will merge within a Hubble time due to GW losses alone (Peters 1964), and thus equations (1a)-(1d) are appropriate.

For AGN with massive accretion disks, it is possible for significant star formation to occur in the region where the disk becomes self-gravitating (Levin & Beloborodov 2003). For standard thin disk models Shakura & Sunyaev (1973), this self-gravitating radius actually corresponds closely to a_h . Since galaxy mergers are often associated with gas inflow and quasar activity, it is quite possible that stars could form in an accretion disk just as a hard BH binary is forming, thereby trapping the stars around the stable Lagrange points. A similar possibility, suggested by Goodman & Tan (2004), is that supermassive stars with $M \gtrsim 10^4 M_\odot$ could grow out of main-sequence seeds embedded in the accretion disk, quickly evolving and then collapsing to intermediate-mass black holes (IMBHs). This scenario is particularly attractive, as it naturally provides a mechanism for making a binary BH with $\mu_2 \lesssim 0.01$ on a circular

orbit, surrounded by ample debris that could easily get trapped into resonant orbits.

Another mechanism that could explain both the low-mass secondary and also provide a supply of stars would be the tidal disruption of a globular cluster by the primary BH. If the globular cluster hosts an IMBH (Miller & Hamilton 2002), it could form a hard binary with the primary, and the surrounding stars could get captured into stable orbits around L_4 and L_5 . At this point, it would be impossible to carry out any quantitative analysis of the relative rates and likelihoods of these different scenarios, considering the remarkable lack of observational evidence for even a single SMBH binary with orbit smaller than a_h . Rather, we might realistically hope to discover such a system with help from one of the EM signatures described below.

4.2. Tidal Disruptions

Tidal disruptions of solar-type stars by SMBHs are expected to occur at a rate of $\sim 10^{-4} \text{ yr}^{-1}$ per MW-type galaxy (Wang & Merritt 2004), and are excellent tools for detecting otherwise-quiescent nuclei at cosmological distances (Lidskii & Ozernoi 1979; Rees 1988). Typical luminosities are comparable to the Eddington limit, and the timescale for the rise and subsequent decay of the light curve is on the order of weeks to months (Ulmer 1999; Halpern et al. 2004), which is ideal for detection by wide-field time-domain surveys such as Pan-STARRS² or LSST³ (Gezari et al. 2009). Tidal disruptions have recently been proposed as tools for detecting BH mergers or recoiling merger remnants, in some cases long after the merger occurs (Komossa & Merritt 2008; Chen et al. 2009; Stone & Loeb 2010).

In our scenario, the main-sequence stars are captured into resonant motion around L_4 or L_5 at large separation ($a \sim a_h$) and then move in closer to the primary as the binary separation slowly shrinks. A star of mass M_* and radius R_* will get disrupted when the tidal forces from the BH are comparable to the star’s own self-gravity, which occurs at a distance R_{td} from the primary:

$$R_{\text{td}} \approx R_* \left(\frac{M_1}{M_*} \right)^{1/3}. \quad (14)$$

In our numerical tests of Section 3, we found that during inspiral, some fraction of test particles get ejected from L_4 or L_5 and disrupted by M_2 , the the majority remain bound until the final merger stage. For stars that remain bound to L_4 or L_5 , the gravitational tidal forces are dominated by the primary, and thus the relevant mass in equation (14) is M_1 .

In Figure 4 we plot the orbital separation of a BH binary as a function of time before merger (*black curves*). The dashed horizontal lines correspond to the points at which (top-to-bottom) an O/B star, a solar-type star, or a white dwarf would get tidally disrupted by the primary BH of mass $10^6 M_\odot$ (*top*) or $10^7 M_\odot$ (*bottom*), and secondary mass $\mu_2 = 0.01$. The vertical dotted lines denote where the binary separation reaches the ISCO and the BHs merge, and the vertical dashed lines correspond to the point where the binary enters the LISA

² <http://pan-starrs.ifa.hawaii.edu>

³ <http://www.lsst.org>

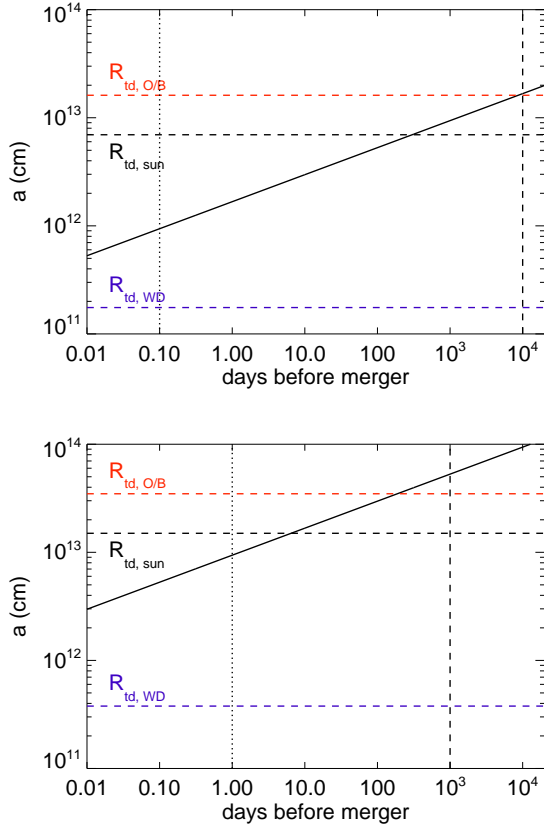


Figure 4. *Upper:* Tidal disruption radius for a star orbiting a $10^6 M_\odot$ BH, as a function of time before merger. The secondary BH has mass $10^4 M_\odot$. *Lower:* Tidal disruption radius for a star orbiting a $10^6 M_\odot$ BH, as a function of time before merger. The secondary BH has mass $10^5 M_\odot$. From top to bottom, the horizontal lines correspond to the tidal disruption radius of a main sequence O/B star, a solar-type star, and a $0.7 M_\odot$ white dwarf. The vertical dotted line corresponds to the point at which the secondary BH reaches the ISCO and the vertical dashed lines the point at which the binary enters the LIGO band ($f_{\text{GW}} \approx 1$ mHz).

GW frequency band. For $M_1 = 10^6 M_\odot$, a solar-type star would get disrupted roughly a year before merger. At that point, LISA would already be able to provide an error-box of ~ 100 square degrees for the source location on the sky (Lang & Hughes 2008), which could be easily monitored for luminous tidal disruption flares out to redshifts $z \sim 0.2$ or so (Gezari et al. 2009). In all cases with $M_1 \gtrsim 10^5 M_\odot$, white dwarfs would not get disrupted, but rather plunge directly into the BH.

In addition to the stars that get disrupted at late times, we saw in the simulations of Section 3 that there are also some particles that get captured by either M_1 or M_2 during the inspiral phase, thus leading to tidal disruption, or get ejected entirely from the system. Table 1 shows the fraction of test particles that meet one of these various fates during inspiral, i.e., when the binary separation is $5M \leq a(t) \leq 35M$. Of course, if equation (14) is met, then even stars on stable orbits are disrupted. As in Figure 3, there are no clear trends with varying μ_2 , but we do confirm that particles around L_5 are generally more likely to get ejected from the system, while particles around L_4 are more likely to get captured or disrupted

Table 1
Fraction of test particles that, during inspiral, are either ejected from the system or captured by one of the BHs.

| | $\mu_2 = 0.01$ | $\mu_2 = 0.02$ | $\mu_2 = 0.038$ |
|-----------------------------|----------------|----------------|-----------------|
| $f(L_4 \rightarrow \infty)$ | 0.13 | 0.11 | 0.13 |
| $f(L_5 \rightarrow \infty)$ | 0.20 | 0.12 | 0.21 |
| $f(L_4 \rightarrow M_1)$ | 0.16 | 0.33 | 0.19 |
| $f(L_5 \rightarrow M_1)$ | 0.15 | 0.05 | 0.10 |
| $f(L_4 \rightarrow M_2)$ | 0.14 | 0.27 | 0.18 |
| $f(L_5 \rightarrow M_2)$ | 0.21 | 0.11 | 0.20 |

by the BHs.

4.3. Ultra-Hyper-Velocity Stars

Of the stars that *do* get ejected from the binary system during inspiral, we find a wide range in their velocities at infinity. To first order, one would expect the ejection velocity to be comparable to the orbital velocity. However, particles ejected at late times when the orbital velocity is highest are also coming from the deepest potentials, so are slowed more as they escape from the system. In practice, we find that net effect is a slight increase in the average escape velocity at late times, but somewhat flatter than the orbital velocity scaling of $a^{-1/2}$. This is likely due to the fact that the most efficient three-body slingshot interactions require the test particle to come within a small fraction of a from the secondary, and when a becomes smaller, these close approaches more likely lead to capture or disruption than ejection.

From equation (14), we see that a solar-type star would get tidally disrupted by a $10^6 M_\odot$ BH at a distance of $\sim 50M$, far outside the ISCO. For $M_1 = 10^7 M_\odot$, however, a star could survive to within $10M$ of the primary. From that separation, we find that test particles are ejected with mean velocities of $0.1c$, roughly 50 times greater than the radial velocities of hyper-velocity stars (HVSs) observed in the outer regions of the Milky Way (Brown et al. 2009). Of course, any star moving that fast would be observable for a much shorter time; only a few million years after the BH merger. At the same time, this allows younger, more massive stars to survive out to the edge of the galaxy, making them even easier to identify against the field stars. It is conceivable that the BH at the center of our galaxy may have experienced a minor merger with $\mu_2 \sim 0.01$ in the past 10 Myr, an event which may be convincingly inferred by the detection of such an ultra-HVS at a distance of $\sim 50 - 100$ kpc.

4.4. Compressed Stellar Systems

In the event that many stars are initially trapped around L_4 or L_5 , the gravitational interactions between the test particles may become important, an effect that we have neglected in this work. Especially for larger systems with $M \gtrsim 10^8 M_\odot$, one could even imagine forming globular clusters around the Lagrange points, although from equation (13) it is clear they would necessarily be quite compact. When the core of a normal globular cluster grows too dense, it can undergo a collapse via gravitational instability, at the same time expanding the orbits of the outer stars, due to conservation of en-

ergy. In our BH binary system, the adiabatic compression of orbits may trigger core collapse of the trapped cluster, while simultaneously preventing any outer stars from escaping, thereby enhancing the stellar density further. If the density becomes high enough, stellar collisions will become common, and the system could act as a breeding ground for supermassive stars and IMBHs (Portegies Zwart et al. 1999).

4.5. Compact Objects

Many of the formation scenarios considered above naturally lead to high-mass stars forming in the dense gaseous environments around the SMBH binary. These stars could then evolve and collapse into neutron stars or stellar-mass BHs on timescales short compared to the inspiral time. Unlike main sequence stars that would get tidally disrupted well before the merger, compact objects would survive unperturbed until they either get ejected or captured whole by one of the BHs. In that case, they would also contribute to the GW signal produced by the binary. For a system with $M_1 = 10^6 M_\odot$, $M_2 = 10^4 M_\odot$, and $m_0 = 10 M_\odot$, the stellar-mass BH would contribute an additional 0.1% to the waveform amplitude. At a distance of 1 Gpc, this small perturbation would still be observable with LISA.

However, if the compact object is orbiting exactly at the L_4 or L_5 with no libration, it would contribute a pure sinusoid component to the waveform with identical frequency as the dominant wave, only with a phase shift of $\pm 120^\circ$. Thus it would be indistinguishable from a normal binary on a circular orbit with slightly different masses and phase. On the other hand, if the compact object is librating with typical amplitude $\Delta\phi \approx 30^\circ$, as we might expect in the general case, the waveform will contain a distinct signal at the libration frequency (in this example, $\omega_{\text{lib}} \approx 0.27\omega_{\text{orb}}$) which may still be detectable. More likely, this extra signal would be confused with a spin-orbit or spin-spin precession frequency, effectively degrading the overall confidence in the binary parameter estimation. In some cases, the stellar-mass BH might get ejected during inspiral, but with small enough velocity that it doesn't escape the system, but rather remains bound on a larger, eccentric orbit even after the two massive BHs merge, ultimately merging much later as an extreme mass-ratio inspiral (EMRI) source.

As mentioned above, the secondary BH and the “test particle” can actually have comparable masses and still maintain stability of the Lagrange points, as long as $\mu_2 \lesssim 0.0385$. Thus a stable three-body BH system could exist with $M_1 \approx 10^6 M_\odot$ and $M_2 \approx M_3 \approx 10^4 M_\odot$, in which case the orbital libration could be seen very clearly in a LISA waveform. The probability of such a system existing is perhaps not as small as one might think, especially if both IMBHs form out of a massive accretion disk, not unlike Saturn's moons Janus and Epimetheus. Indeed, only 15 years ago, the possibility of “Hot Jupiters” with $\mu_2 \gtrsim 0.001$, orbiting very close to their host stars was considered quite remote, and now we know of hundreds of such systems. The same may very well be true of SMBHs and their surrounding gas disks.

4.6. Diffuse Gas

In the circumbinary accretion disk model, ample gas and dust will surround the BH binary, of which some

fraction could likely get trapped into orbits around L_4 and L_5 . If cold enough, this gas could get compressed by the evolving binary potential and form stars or even clusters of stars, as discussed above. More likely, the gas will be rather hot, with thermal velocities comparable to the libration velocities of test particles filling the stable volume around L_4 and L_5 . One very rough estimate of this thermal motion may come from inspection of equation (2) and Figure 1. Trapped particles will have $C_{J0}(L_4) \lesssim C_J \lesssim C_{J0}(L_3)$, so typical velocities in the rotating frame of

$$v^2 \approx C_J(L_3, v=0) - C_J(L_4, v=0) \approx 2\mu_2 a^{-1} \quad (15)$$

(Murray & Dermott 1999). Combining with equation (13) for the separation at the time of binary formation, we get an initial thermal velocity of

$$v_{\text{therm}} \approx 600 \text{ km s}^{-1} \left(\frac{\sigma}{200 \text{ km s}^{-1}} \right), \quad (16)$$

or roughly 4×10^7 K. Somewhat remarkably, v_{therm} is independent of μ_2 or M_1 (except indirectly through the $M - \sigma$ relationship).

We can estimate an upper limit on the density of this gas ρ_0 by requiring it to be stable to gravitational collapse. In other words, the total mass should not exceed the Jeans mass:

$$0.005 \rho_0 a_h^3 \leq \left(\frac{5k_B T}{Gm_p} \right)^{3/2} \left(\frac{3}{4\pi\rho_0} \right)^{1/2}, \quad (17)$$

with k_B the Boltzmann constant and m_p the proton mass. The leading factor of 0.005 comes from the volume of the stable region, estimated from Figure 3. Taking $m_p v_{\text{therm}}^2 = 3k_B T$, we get

$$\rho_0 \leq 35 \left(\frac{v_{\text{therm}}^2}{G a_h^2} \right), \quad (18)$$

corresponding to a total mass in gas of

$$M_{\text{gas}} \approx 0.005 \rho_0 a_h^3 \leq 7 \times 10^4 M_\odot \left(\frac{\mu_2}{0.02} \right) \left(\frac{M}{10^7 M_\odot} \right), \quad (19)$$

which is far more than enough material to fuel a bright EM counterpart.

Even if the density of the trapped gas is orders of magnitude smaller, it should still be sufficient to produce observable emission lines if irradiated by an AGN or quasar powered by accretion onto one of the BHs. For a cloud of gas filling the stable region around each Lagrange point, the covering fraction would be on the order of a few percent. Since the thermal velocity is roughly a factor of 10 smaller than the orbital velocity, the emission lines would be somewhat narrower than a classical broad line originating from the same radius. The coherent shape and motion of the cloud would also give rise to a large velocity offset relative to the host galaxy or narrow emission line clouds residing at a greater distance from the central engine. This offset in wavelength would vary periodically with the binary orbit (T_{orb} at our fiducial value of a_h would be on the order of 10 years), giving strong evidence for the existence of a BH binary. Such an effect could be detected by large spectroscopic surveys like

the Sloan Digital Sky Survey, a technique already in frequent use by observers searching for binary quasars or recoiling black holes (Bonning et al. 2007; Komossa et al. 2008; Boroson & Lauer 2009)

5. DISCUSSION

We have analyzed the circular restricted three-body problem including leading-order terms for gravitational wave losses, in particular studying the behavior of test particle orbits near the stable Lagrange points L_4 and L_5 . We find that these orbits remain stable throughout most of the adiabatic inspiral phase, and their locations shift relative to the Newtonian limit as the binary enters the late phases of inspiral and merger. Analogous to the case of inertial drag forces in the planetary problem, the non-conservative GW loss terms lead to an asymmetry between L_4 and L_5 : test particles around L_4 move closer to the secondary BH, while those initially around L_5 move away from it. While there appear to be complicating resonances that affect the relative stability of the two regions differently for different mass ratios, a general trend is that the inclusion of GW losses increases the stability of L_5 while decreasing the stability of L_4 . Particles initially around L_4 are more likely than those around L_5 to get captured or disrupted by M_2 , while particles near L_5 are more likely to get ejected from the system entirely. However, in both cases, the vast majority of particles get neither ejected nor captured until the binary separation is on the order $a \lesssim 5M$, at which point the Newtonian equations of motion break down entirely and everything plunges into the primary BH.

The stability of the L_4 and L_5 Lagrange points throughout most of the inspiral provides a natural mechanism for shepherding material from relatively large radii down to the central BH, in turn producing a luminous EM counterpart to the GW signal from a BH merger. The detailed physics behind such an EM signal are well beyond the scope of this paper, but early results from numerical relativity simulations suggest that bright EM flares should be quite general, provided enough gas is available (van Meter et al. 2010; Bode et al. 2010; Farris et al. 2010). In addition to the prompt emission associated with the final merger, we have shown that hyper-velocity stars with speeds as high as $0.1c$ might be observable, flying away from the galactic center for millions of years after the merger. With sufficient column densities of diffuse gas trapped around L_4 and L_5 , a precursor signal could take the form of highly red/blue-shifted emission lines, narrower than typical broad lines, with the line offset varying periodically with the BH orbit.

For the majority of the results in this paper, we require that the secondary mass be relatively small: $\mu_2 \leq 0.0385$ to guarantee linear stability of L_4 and L_5 . It is unclear how common BH binaries with such mass ratios might be, and whether they are more likely to form via galactic mergers or *in situ*, via the collapse of supermassive stars, accretion from a surrounding disk, or capture from a tidally stripped globular cluster. However, there are other resonances in the restricted three-body problem that may lead to qualitatively similar behavior: the stable transport of matter from large radii down to the ISCO at the time of merger. One example from the solar system is the Hilda family of asteroids that occupy stable

eccentric orbits with periods $2/3$ that of Jupiter. This ensures that they avoid close encounters with Jupiter at apocenter, where they spend most of their time. In the corotating frame, a snapshot of their positions will appear to fill out a triangle with vertices aligned with L_3 , L_4 , and L_5 (Brož & Vokrouhlický 2008). Guéron (2006) showed that this resonance is stable even in the extreme relativistic limit, but still with small mass ratios ($\mu_2 \approx 0.001$). Our own preliminary results suggest that this $2 : 3$ resonance is linearly stable for mass ratios at least as large as $\mu_2 \approx 0.1$, but we leave a comprehensive study of the problem, including GW losses, to a future paper.

In addition to all the Newtonian resonance behavior present in the three-body problem, the two BHs may also get locked into spin-orbital resonances with each other during inspiral (Schittman 2004). Coupled with the non-degenerate orbital frequencies of test particles in a Kerr background, the inclusion of spinning BHs would introduce many new degrees of freedom that may affect the stability of L_4 and L_5 . While we do not think additional PN terms in the equations of motion will significantly change our results on a qualitative level, future work that addresses these questions in more detail is certainly warranted.

The author would like to thank Doug Hamilton, Matthew Holman, Scott Hughes, Julian Krolik, David Merritt, and Cole Miller for helpful discussions and comments. This work was supported by the Chandra Postdoctoral Fellowship Program.

REFERENCES

- Armitage, P. J., & Natarajan, P. 2002, ApJ 567, L9.
- Artymowicz, P., & Lubow, S. H. 1994, ApJ 421, 651.
- Artymowicz, P., & Lubow, S. H. 1996, ApJ 467, L77.
- Bloom, J. S. 2009, White paper for Astro2010 Decadal Survey, [arXiv:0902.1527].
- Bode, T., Haas, R., Bogdanovic, T., Laguna, P., & Shoemaker, D. 2010, ApJ 715, 1117.
- Bonning, E. W., Shields, G. A., & Salviander, S. 2007, ApJ 666, L13.
- Boroson, T. A., & Lauer, T. R. 2009, Nature 458, 53.
- Brown, W. R., Geller, M. J., & Kenyon, S. J. 2009, ApJ 690, 1639.
- Brož, M., & Vokrouhlický, D. 2008, MNRAS 390, 715.
- Buonanno, A., Iyer, B. R., Ochsner, E., Pan, Y., & Sathyaprakash, B. S. 2009, Phys. Rev. D 80, 084043.
- Chang, P., Strubbe, L. E., Menou, K., & Quataert, E. 2009, [arXiv:0906.0825].
- Chen, X., Madau, P., Sesana, A., & Liu, F. K. 2009, ApJ 697, L149.
- Deprit, A., & Deprit-Batholomé, A. 1967, AJ 72, 173.
- Erdi, B., Forgacs-Dajka, E., Nagy, I., & Rajnai, R. 2009, Celest. Mech. Dyn. Astr. 104, 145.
- Farris, B. D., Liu, Y.-K., & Shapiro, S. L. 2010, Phys. Rev. D 81, 084008.
- Fleming, H. J., & Hamilton, D. P. 2000, Icarus 148, 479.
- Gezari, S., et al. 2009, ApJ 698, 1367.
- Goodman, J., & Tan, J. C. 2004, ApJ 608, 108.
- Guéron, E. 2006, Class. Quantum Grav. 23, 673.
- Halpern, J. P., Gezari, S., & Komossa, S. 2004, ApJ 604, 572.
- Hopman, C., & Alexander, T. 2006, ApJ 645, 1152.
- Kary, D. M., & Lissauer, J. J. 1995, Icarus 177, 1.
- Komossa, S., & Merritt, D. 2008, ApJ 683, L21.
- Komossa, S., Zhou, H., & Lu, H. 2008, ApJ 678, L81.
- Krolik, J. H. 2010, ApJ 709, 774.
- Lang, R. N., & Hughes, S. A. 2008, ApJ 677, 1184.
- Levin, Y., & Beloborodov, A. M. 2003, ApJ 590, L33.

- Lidskii, V. V., & Ozernoi, G. M. 1979, *AZh. Pis'ma* 5, 28
(English transl. in *Sov. Astron. Lett.* 5, 16).
- O'Neill, S. M., Miller, M. C., Bogdanovic, T., Reynolds, C. S., & Schnittman, J. D. 2009, *ApJ* 700, 859.
- Marzari, F., & Scholl, H. 1998, *Icarus* 131, 41.
- Merritt, D. 2006, *ApJ* 648, 946.
- Miller, M. C., & Hamilton, D. P. 2002, *MNRAS* 330, 232.
- Milosavljevic, M., & Phinney, E. S. 2005, *ApJ* 622, L93.
- Mosta, P., Palenzuela, C., Rezzolla, L., Lehner, L., Yoshida, S., Pollney, D. 2010, *Phys. Rev. D* 81, 064017.
- Murray, C. D. 1994, *Icarus* 112, 465.
- Murray, C. D., & Dermott, S. F. 1999, *Solar System Dynamics*, Cambridge University Press, Cambridge.
- Palenzuela, C., Anderson, M., Lehner, L., Liebling, S. L., & Neilsen, D. 2009, *Phys. Rev. Lett.* 103, 081101.
- Palenzuela, C., Lehner, L., & Yoshida, S. 2010, *Phys. Rev. D* 81, 084007.
- Peters, P. C. 1964, *Phys. Rev.* 136, 1224.
- Portegies Zwart, S. F., Makino, J., McMillan, S. L. W., & Hut, P. 1999, *A & A* 348, 117.
- Pringle, J. E. 1991, *MNRAS* 248, 754.
- Rabe, E. 1972, in *Motion, Evolution of Orbits, and Origin of Comets. Proceedings of 45th IAU Symposium*, pp. 55-60. Springer-Verlag, New York/Berlin.
- Rees, M. 1988, *Nature* 333, 523.
- Rosswog, S., & Trautman, D. 1996, *Plant. Space Sci.* 44, 313.
- Salo, H., & Yoder, C. F. 1988, *A&A* 205, 309.
- Schnittman, J. D. 2004, *Phys. Rev. D*, 124020.
- Seto, N., & Muto, T. 2010, *Phys. Rev. D*, in press. [arXiv:1005.3114].
- Shakura, N. I., & Sunyaev, R. A. 1973, *A&A*, 24, 337
- Shoemaker, E. M., Shoemaker, C. S., & Wolfe, R. F. 1989, in *Asteroids II*, pp. 487-523. Univ. of Arizona Press, Tucson.
- Stone, N., & Loeb, A. 2010, [arXiv:1004.4833].
- Ulmer, A. 1999, *ApJ* 514, 180.
- van Meter, J. R., Wise, J. H., Miller, M. C., Reynolds, C. S., Centrella, J., Baker, J. G., Boggs, W. D., Kelly, B. J., & McWilliams, S. T. 2010, *ApJ* 711, L89.
- Wang, J., & Merritt, D. 2004, *ApJ* 600, 149.
- Yoder, C. F. 1979, *Icarus* 40, 341.